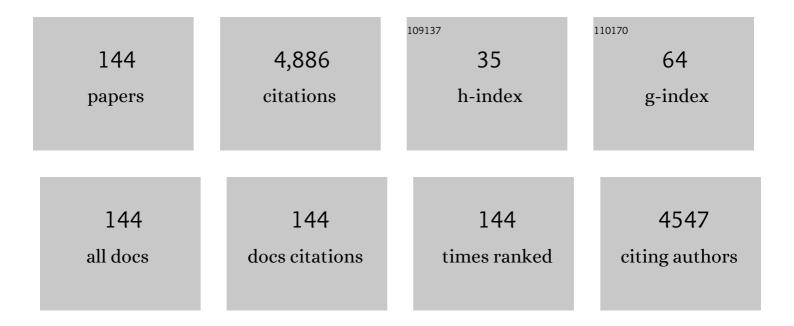
List of Publications by Year in descending order

Source: https://exaly.com/author-pdf/8868998/publications.pdf

Version: 2024-02-01



#	Article	IF	CITATIONS
1	PLOSL: Population learning followed by one shot learning pulmonary image registration using tissue volume preserving and vesselness constraints. Medical Image Analysis, 2022, 79, 102434.	7.0	6
2	Contact mechanics model of lung lobar sliding. Applications in Engineering Science, 2022, 10, 100098.	0.5	2
3	Quantitative CT Characteristics of Cluster Phenotypes in the Severe Asthma Research Program Cohorts. Radiology, 2022, 304, 450-459.	3.6	3
4	Single Volume Lung Biomechanics from Chest Computed Tomography Using a Mode Preserving Generative Adversarial Network. , 2022, , .		1
5	Computed Tomography–based Airway Surface Area–to-Volume Ratio for Phenotyping Airway Remodeling in Chronic Obstructive Pulmonary Disease. American Journal of Respiratory and Critical Care Medicine, 2021, 203, 185-191.	2.5	17
6	CT image segmentation for inflamed and fibrotic lungs using a multi-resolution convolutional neural network. Scientific Reports, 2021, 11, 1455.	1.6	32
7	Regional Gas Transport During Conventional and Oscillatory Ventilation Assessed by Xenon-Enhanced Computed Tomography. Annals of Biomedical Engineering, 2021, 49, 2377-2388.	1.3	5
8	Radiation-induced Hounsfield unit change correlates with dynamic CT perfusion better than 4DCT-based ventilation measures in a novel-swine model. Scientific Reports, 2021, 11, 13156.	1.6	7
9	Effects of Lung Injury on Regional Aeration and Expiratory Time Constants: Insights From Four-Dimensional Computed Tomography Image Registration. Frontiers in Physiology, 2021, 12, 707119.	1.3	11
10	Geodesic density regression for correcting 4DCT pulmonary respiratory motion artifacts. Medical Image Analysis, 2021, 72, 102140.	7.0	8
11	Case Studies in Physiology: Temporal variations of the lung parenchyma and vasculature in asymptomatic COVID-19 pneumonia: a multispectral CT assessment. Journal of Applied Physiology, 2021, 131, 454-463.	1.2	5
12	Radiation-induced airway changes and downstream ventilation decline in a swine model. Biomedical Physics and Engineering Express, 2021, 7, 065039.	0.6	7
13	Multi-resolution convolutional neural networks for fully automated segmentation of acutely injured lungs in multiple species. Medical Image Analysis, 2020, 60, 101592.	7.0	55
14	N-Phase Local Expansion Ratio for Characterizing Out-of-Phase Lung Ventilation. IEEE Transactions on Medical Imaging, 2020, 39, 2025-2034.	5.4	12
15	A Deep Learning Approach to Video Fluoroscopic Swallowing Exam Classification. , 2020, , .		3
16	Modeling the impact of outâ€ofâ€phase ventilation on normal lung tissue response to radiation dose. Medical Physics, 2020, 47, 3233-3242.	1.6	10
17	Quantifying Regional Lung Deformation Using Four-Dimensional Computed Tomography: A Comparison of Conventional and Oscillatory Ventilation. Frontiers in Physiology, 2020, 11, 14.	1.3	15
18	Deep neural network analyses of spirometry for structural phenotyping of chronic obstructive pulmonary disease. JCI Insight, 2020, 5, .	2.3	23

#	Article	IF	CITATIONS
19	Registration-Invariant Biomechanical Features for Disease Staging of COPD in SPIROMICS. Lecture Notes in Computer Science, 2020, , 143-154.	1.0	3
20	FissureNet: A Deep Learning Approach For Pulmonary Fissure Detection in CT Images. IEEE Transactions on Medical Imaging, 2019, 38, 156-166.	5.4	77
21	Pulmonary Lobe Segmentation Using A Sequence of Convolutional Neural Networks For Marginal Learning. , 2019, , .		18
22	The VAMPIRE challenge: A multiâ€institutional validation study of CT ventilation imaging. Medical Physics, 2019, 46, 1198-1217.	1.6	59
23	A Novel Method for Automatic Identification of Breathing State. Scientific Reports, 2019, 9, 103.	1.6	13
24	Recent Advances in Computed Tomography Imaging in Chronic Obstructive Pulmonary Disease. Annals of the American Thoracic Society, 2018, 15, 281-289.	1.5	44
25	Detecting Out-of-Phase Ventilation Using 4DCT to Improve Radiation Therapy for Lung Cancer. Lecture Notes in Computer Science, 2018, , 251-259.	1.0	2
26	Quantifying ventilation change due to radiation therapy using 4 <scp>DCT</scp> Jacobian calculations. Medical Physics, 2018, 45, 4483-4492.	1.6	22
27	Transfer Learning for Segmentation of Injured Lungs Using Coarse-to-Fine Convolutional Neural Networks. Lecture Notes in Computer Science, 2018, , 191-201.	1.0	4
28	Airway fractal dimension predicts respiratory morbidity and mortality in COPD. Journal of Clinical Investigation, 2018, 128, 5374-5382.	3.9	38
29	Biomechanical CT metrics are associated with patient outcomes in COPD. Thorax, 2017, 72, 409-414.	2.7	41
30	Computed Tomography Measure of Lung at Risk and Lung Function Decline in Chronic Obstructive Pulmonary Disease. American Journal of Respiratory and Critical Care Medicine, 2017, 196, 569-576.	2.5	59
31	Signs of Gas Trapping in Normal Lung Density Regions in Smokers. American Journal of Respiratory and Critical Care Medicine, 2017, 196, 1404-1410.	2.5	26
32	Computed Tomography Image Matching in Chronic Obstructive Pulmonary Disease. Critical Reviews in Biomedical Engineering, 2016, 44, 411-425.	0.5	2
33	Tissue-Volume Preserving Deformable Image Registration for 4DCT Pulmonary Images. , 2016, , .		4
34	Current-and Varifold-Based Registration of Lung Vessel and Airway Trees. , 2016, , .		3
35	Evaluation of the ΔV 4D CT ventilation calculation method using <i>in vivo</i> xenon CT ventilation data and comparison to other methods. Journal of Applied Clinical Medical Physics, 2016, 17, 550-560.	0.8	11
36	CT-derived Biomechanical Metrics Improve Agreement Between Spirometry and Emphysema. Academic Radiology, 2016, 23, 1255-1263.	1.3	26

#	Article	IF	CITATIONS
37	Automated Method for Identification and Artery-Venous Classification of Vessel Trees in Retinal Vessel Networks. PLoS ONE, 2014, 9, e88061.	1.1	66
38	A Measure for Characterizing Sliding on Lung Boundaries. Annals of Biomedical Engineering, 2014, 42, 642-650.	1.3	20
39	Quantification of confocal images of biofilms grown on irregular surfaces. Journal of Microbiological Methods, 2014, 100, 111-120.	0.7	20
40	Development of a preliminary pediatric tracheal growth model from magnetic resonance images. Laryngoscope, 2014, 124, 1947-1951.	1.1	6
41	Registration-Based Lung Mechanical Analysis of Chronic Obstructive Pulmonary Disease (COPD) Using a Supervised Machine Learning Framework. Academic Radiology, 2013, 20, 527-536.	1.3	57
42	Splat Feature Classification With Application to Retinal Hemorrhage Detection in Fundus Images. IEEE Transactions on Medical Imaging, 2013, 32, 364-375.	5.4	147
43	Graph-based segmentation of the pediatric trachea in MR images to model growth. Proceedings of SPIE, 2013, , .	0.8	0
44	Air Trapping and Airflow Obstruction in Newborn Cystic Fibrosis Piglets. American Journal of Respiratory and Critical Care Medicine, 2013, 188, 1434-1441.	2.5	60
45	Respiratory effort correction strategies to improve the reproducibility of lung expansion measurements. Medical Physics, 2013, 40, 123504.	1.6	28
46	Reproducibility of intensityâ€based estimates of lung ventilation. Medical Physics, 2013, 40, 063504.	1.6	21
47	Intensity-Based Registration for Lung MotionÂEstimation. Biological and Medical Physics Series, 2013, , 125-158.	0.3	1
48	Estimation of Lung Ventilation. Biological and Medical Physics Series, 2013, , 297-317.	0.3	0
49	Tracking Regional Tissue Volume and Function Change in Lung Using Image Registration. International Journal of Biomedical Imaging, 2012, 2012, 1-14.	3.0	6
50	Improving Intensity-Based Lung CT Registration Accuracy Utilizing Vascular Information. International Journal of Biomedical Imaging, 2012, 2012, 1-17.	3.0	21
51	Automated Detection of Malarial Retinopathy-Associated Retinal Hemorrhages. , 2012, 53, 6582.		21
52	Automated artery-venous classification of retinal blood vessels based on structural mapping method. Proceedings of SPIE, 2012, , .	0.8	10
53	Retinal vessel width measurement at branching points using an improved electric field theory-based graph approach. Proceedings of SPIE, 2012, , .	0.8	2
54	Reproducibility of registration-based measures of lung tissue expansion. Medical Physics, 2012, 39, 1595-1608.	1.6	55

#	Article	IF	CITATIONS
55	Comparison of image registration based measures of regional lung ventilation from dynamic spiral CT with Xeâ€CT. Medical Physics, 2012, 39, 5084-5098.	1.6	55
56	Estimation of lung lobar sliding using image registration. , 2012, , .		1
57	Establishing a Normative Atlas of the Human Lung. Academic Radiology, 2012, 19, 1368-1381.	1.3	27
58	Enhanced analysis of bacteria susceptibility in connected biofilms. Journal of Microbiological Methods, 2012, 90, 9-14.	0.7	4
59	Extraction of Airways From CT (EXACT'09). IEEE Transactions on Medical Imaging, 2012, 31, 2093-2107.	5.4	173
60	Retinal Vessel Width Measurement at Branchings Using an Improved Electric Field Theory-Based Graph Approach. PLoS ONE, 2012, 7, e49668.	1.1	5
61	Segmentation of pathological and diseased lung tissue in CT images using a graph-search algorithm. , 2011, , .		46
62	Effect of Segmental Bronchoalveolar Lavage on Quantitative Computed Tomography of the Lung. Academic Radiology, 2011, 18, 876-884.	1.3	8
63	Automated method for the identification and analysis of vascular tree structures in retinal vessel network. Proceedings of SPIE, 2011, , .	0.8	12
64	Three-dimensional characterization of regional lung deformation. Journal of Biomechanics, 2011, 44, 2489-2495.	0.9	69
65	Vessel Boundary Delineation on Fundus Images Using Graph-Based Approach. IEEE Transactions on Medical Imaging, 2011, 30, 1184-1191.	5.4	93
66	Evaluation of Registration Methods on Thoracic CT: The EMPIRE10 Challenge. IEEE Transactions on Medical Imaging, 2011, 30, 1901-1920.	5.4	363
67	A cubic B-spline-based hybrid registration of lung CT images for a dynamic airway geometric model with large deformation. Physics in Medicine and Biology, 2011, 56, 203-218.	1.6	49
68	Registration-based measurement of regional expiration volume ratio using dynamic 4DCT imaging. , 2011, , .		4
69	Time-varying lung ventilation analysis of 4DCT using image registration. , 2011, , .		0
70	Identification and reconnection of interrupted vessels in retinal vessel segmentation. , 2011, , .		13
71	Simultaneous automatic detection of optic disc and fovea on fundus photographs. , 2011, , .		4
72	Human airway tree structure query atlas. Proceedings of SPIE, 2010, , .	0.8	0

#	Article	IF	CITATIONS
73	Lung structure phenotype variation in inbred mouse strains revealed through in vivo micro-CT imaging. Journal of Applied Physiology, 2010, 109, 1960-1968.	1.2	74
74	Computer-Assisted Assessment of Hyoid Bone Motion from Videofluoroscopic Swallow Studies. Dysphagia, 2010, 25, 298-306.	1.0	37
75	Objective and expert-independent validation of retinal image registration algorithms by a projective imaging distortion model. Medical Image Analysis, 2010, 14, 539-549.	7.0	22
76	Automated measurement of retinal blood vessel tortuosity. Proceedings of SPIE, 2010, , .	0.8	13
77	4DCTâ€based measurement of changes in pulmonary function following a course of radiation therapy. Medical Physics, 2010, 37, 1261-1272.	1.6	89
78	Retinal atlas statistics from color fundus images. Proceedings of SPIE, 2010, , .	0.8	9
79	Automated Quantification of Inherited Phenotypes from Color Images: A Twin Study of the Variability of Optic Nerve Head Shape. , 2010, 51, 5870.		8
80	Automated Early Detection of Diabetic Retinopathy. Ophthalmology, 2010, 117, 1147-1154.	2.5	221
81	A Process Model for Direct Correlation between Computed Tomography and Histopathology. Academic Radiology, 2010, 17, 169-180.	1.3	7
82	Tissue volume and vesselness measure preserving nonrigid registration of lung CT images. Proceedings of SPIE, 2010, , .	0.8	17
83	Unifying Vascular Information in Intensity-Based Nonrigid Lung CT Registration. Lecture Notes in Computer Science, 2010, , 1-12.	1.0	9
84	A Novel Method of Characterizing Regional Lung Deformation. , 2010, , .		0
85	Engineering patient-specific drill templates and bioabsorbable posterior cervical plates: a feasibility study. Journal of Neurosurgery: Spine, 2009, 10, 129-132.	0.9	20
86	Image-based drill templates for cervical pedicle screw placement. Journal of Neurosurgery: Spine, 2009, 10, 21-26.	0.9	46
87	Registration-based regional lung mechanical analysis: retrospectively reconstructed dynamic imaging versus static breath-hold image acquisition. Proceedings of SPIE, 2009, , .	0.8	10
88	Anatomy-Guided Lung Lobe Segmentation in X-Ray CT Images. IEEE Transactions on Medical Imaging, 2009, 28, 202-214.	5.4	127
89	An Airway Phantom to Standardize CT Acquisition in Multicenter Clinical Trials. Academic Radiology, 2009, 16, 1134-1141.e1.	1.3	14
90	Evaluation of Lobar Biomechanics during Respiration Using Image Registration. Lecture Notes in Computer Science, 2009, 12, 739-746.	1.0	28

#	Article	IF	CITATIONS
91	Comparison of Regional Lung Deformation Between Dynamic and Static CT Imagery Using Inverse Consistent Registration. , 2009, , .		0
92	Registration-based estimates of local lung tissue expansion compared to xenon CT measures of specific ventilation. Medical Image Analysis, 2008, 12, 752-763.	7.0	273
93	Integrated CT/Bronchoscopy in the Central Airways. Academic Radiology, 2008, 15, 786-798.	1.3	17
94	Retinal image mosaicing using the radial distortion correction model. , 2008, , .		9
95	CT-measured regional specific volume change reflects regional ventilation in supine sheep. Journal of Applied Physiology, 2008, 104, 1177-1184.	1.2	97
96	Tracking the hyoid bone in videofluoroscopic swallowing studies. , 2008, , .		1
97	Pulmonary CT image registration and warping for tracking tissue deformation during the respiratory cycle through 3D consistent image registration. Medical Physics, 2008, 35, 5575-5583.	1.6	25
98	GUEST EDITORIAL: MEDICAL IMAGING INFORMATICS — AN INFORMATION PROCESSING FROM IMAGE FORMATION TO VISUALIZATION. International Journal of Image and Graphics, 2007, 07, 1-15.	1.2	2
99	Validation of Retinal Image Registration Algorithms by a Projective Imaging Distortion Model. Annual International Conference of the IEEE Engineering in Medicine and Biology Society, 2007, 2007, 6472-5.	0.5	12
100	Feature-based pairwise retinal image registration by radial distortion correction. , 2007, , .		10
101	Rapid prototype patient-specific drill template for cervical pedicle screw placement. Computer Aided Surgery, 2007, 12, 303-308.	1.8	72
102	Three-dimensional murine airway segmentation in micro-CT images. , 2007, , .		4
103	Breast MRI lesion classification: Improved performance of human readers with a backpropagation neural network computer-aided diagnosis (CAD) system. Journal of Magnetic Resonance Imaging, 2007, 25, 89-95.	1.9	138
104	Registration-Derived Estimates of Local Lung Expansion as Surrogates for Regional Ventilation. Lecture Notes in Computer Science, 2007, 20, 763-774.	1.0	27
105	Rapid prototype patient-specific drill template for cervical pedicle screw placement. Computer Aided Surgery, 2007, 12, 303-308.	1.8	10
106	Atlas-driven lung lobe segmentation in volumetric X-ray CT images. IEEE Transactions on Medical Imaging, 2006, 25, 1-16.	5.4	170
107	Establishing multimodality datasets with the incorporation of 3D histopathology for soft tissue classification. , 2006, , .		2
108	Automatic segmentation of pulmonary fissures in x-ray CT images using anatomic guidance. , 2006, , .		5

Automatic segmentation of pulmonary fissures in x-ray CT images using anatomic guidance. , 2006, , . 108

#	Article	IF	CITATIONS
109	3D pulmonary airway color image reconstruction via shape from shading and virtual bronchoscopy imaging techniques. , 2005, , .		2
110	Classification of pulmonary airway disease based on mucosal color analysis. , 2005, , .		1
111	Virtual bronchoscopy for quantitative airway analysis. , 2005, , .		13
112	Three-dimensional visual truth of the normal airway tree for use as a quantitative comparison to micro-CT reconstructions. , 2005, , .		5
113	The use and benefit of stereology in choosing a CT scanning protocol for the lung. , 2005, 5747, 667.		0
114	Estimation of regional lung expansion via 3D image registration. , 2005, , .		6
115	Automatic lung lobe segmentation in x-ray CT images by 3D watershed transform using anatomic information from the segmented airway tree. , 2005, , .		13
116	Macro-optical color assessment of the pulmonary airways with subsequent three-dimensional multidetector-x-ray-computed-tomography assisted display. Journal of Biomedical Optics, 2005, 10, 051703.	1.4	9
117	Computed Tomography Studies of Lung Mechanics. Proceedings of the American Thoracic Society, 2005, 2, 517-521.	3.5	37
118	Smoothing Lung Segmentation Surfaces in Three-dimensional X-ray CT Images Using Anatomic Guidance1. Academic Radiology, 2005, 12, 1502-1511.	1.3	28
119	Cardiac Image Processing. , 2005, , 1175-XXXIV.		1
120	Smoothing lung segmentation surfaces in 3D x-ray CT images using anatomic guidance. , 2004, 5370, 1066.		20
121	The comprehensive imaging-based analysis of the lung. Academic Radiology, 2004, 11, 1370-1380.	1.3	67
122	Segmentation of the ovine lung in 3D CT Images. , 2004, , .		2
123	Three-dimensional true color topographical analysis of the pulmonary airways. , 2004, 5369, 189.		5
124	A whole organ serial sectioning and imaging system for correlation of pathology to computer tomography. , 2004, 5324, 224.		4
125	Characterization of the interstitial lung diseases via density-based and texture-based analysis of computed tomography images of lung structure and function1. Academic Radiology, 2003, 10, 1104-1118.	1.3	179
126	Establishing a Normative Atlas of the Human Lung. Academic Radiology, 2003, 10, 255-265.	1.3	124

JOSEPH M REINHARDT

#	Article	IF	CITATIONS
127	Segmentation and analysis of the human airway tree from three-dimensional X-ray CT images. IEEE Transactions on Medical Imaging, 2003, 22, 940-950.	5.4	202
128	Atlas-driven lung lobe segmentation in volumetric x-ray CT images. , 2003, , .		11
129	Classification of mammographic masses: comparison between Backpropagation Neural Network (BNN) and human readers. , 2003, , .		2
130	Maximizing quantitative accuracy of lung airway lumen and wall measures obtained from X-ray CT imaging. Journal of Applied Physiology, 2003, 95, 1063-1075.	1.2	109
131	3D human airway segmentation for virtual bronchoscopy. , 2002, 4683, 16.		12
132	3D intersubject warping and registration of pulmonary CT images for a human lung model. , 2002, 4683, 324.		8
133	Three-Dimensional Human Airway Segmentation Methods for Clinical Virtual Bronchoscopy. Academic Radiology, 2002, 9, 1153-1168.	1.3	141
134	Color analysis of the human airway wall. , 2002, , .		0
135	<title>Lung lobe segmentation by graph search with 3D shape constraints</title> . , 2001, , .		29
136	<title>Evaluation and application of 3D lung warping and registration model using HRCT images</title> ., 2001, 4321, 234.		22
137	<title>Automatic generation of object shape models and their application to tomographic image segmentation</title> ., 2001, , .		12
138	<title>Computed tomographic-based estimation of airway size with correction for scanned plane tilt
angle</title> . , 2000, , .		4
139	Cue-Based Segmentation of 4D Cardiac Image Sequences. Computer Vision and Image Understanding, 2000, 77, 251-262.	3.0	5
140	<title>3D pulmonary CT image registration with a standard lung atlas</title> ., 2000, 3978, 67.		11
141	<title>Detection of lung lobar fissures using fuzzy logic</title> . , 1999, , .		17
142	Quantitative pulmonary imaging: Spatial and temporal considerations in high-resolution CT. Academic Radiology, 1998, 5, 539-546.	1.3	14
143	<title>Automatic axis generation for 3D virtual-bronchoscopic image assessment</title> . , 1998, , .		3
144	<title>Flexible search-based approach for morphological shape decomposition</title> . , 1993, 2094, 1424.		2